metals

MDPI

Article

Single-Pass Process of Square Butt Joints without Edge Preparation Using Hot-Wire Gas Metal Arc Welding

Nattasak Suwannatee and Motomichi Yamamoto *

Graduate School of Advanced Science and Engineering, Hiroshima University, Higashi-Hiroshima 730-0046, Japan; d205056@hiroshima-u.ac.jp
* Correspondence: motoyama@hiroshima-u.ac.jp; Tel.: +81-82-424-7815

Abstract: This paper presents a novel approach to welding thick steel plates that offers time and energy savings compared with conventional techniques. The combination of gas metal arc welding (GMAW) and hot-wire technology simplifies the joint configuration and enhances the process tolerance. In this study, a square butt joint was prepared with as-cut edges and a thickness of 15 mm. The relationship between the welding current and the deposition rate of solo GMAW showed limitations and low process tolerance. Increasing the welding current led to a larger deposited volume with unnecessary weld penetration. An independent deposition volume due to hot-wire insertion was used to improve process tolerance. This approach provided an additional volume without increasing the welding current and reduced unnecessary penetration. With optimized parameters, full-penetration single-pass welding was achieved. Compared with the formation of a typical single-v butt joint at a similar welding speed of 30 cm/min, the proposed process reduced the minimum arc time and power consumption by approximately 83% and 62%, respectively. Moreover, a single pass at a travel speed of 60 cm/min was achieved with approximately 91% and 81% less arc time and power consumption, respectively. In summary, the combined process simplifies the joint configuration, enables full-penetration single-pass welding, and reduces time and energy requirements.

Keywords: hot-wire; gas metal arc welding; single-pass welding; lower energy consumption welding

check for updates

Citation: Suwannatee, N.; Yamamoto, M. Single-Pass Process of Square Butt Joints without Edge Preparation Using Hot-Wire Gas Metal Arc Welding. *Metals* **2023**, *13*, 1014. https://doi.org/10.3390/met13061014

Academic Editor: António Bastos Pereira

Received: 8 May 2023
Revised: 21 May 2023
Accepted: 22 May 2023
Published: 24 May 2023

Copyright: © 2023 by the authors. Licensee MDPI, Basel, Switzerland. This article is an open access article distributed under the terms and conditions of the Creative Commons Attribution (CC BY) license (https://creativecommons.org/licenses/by/4.0/).

1. Introduction

Traditional welding processes, including gas metal arc welding (GMAW), necessitate the preparation of grooves (edges) to ensure the accessibility of a welding torch and produce high-quality welds without defects. However, the joint preparation process is not only time-consuming but also expensive [1,2]. Moreover, a large groove area requires many welding passes and/or high welding current in GMAW to achieve the desired deposition volume. For example, conventional GMAW typically requires a minimum of 41 weld passes to create a bevel groove outside corner joint on a 100 mm thick steel plate [3]. Additionally, a welding technique utilizing high current with carbon dioxide as a shielding gas requires welding current ranging from 400 to 600 A at 30 cm/min of travel speed [4–6]. In order to increase productivity, highly efficient welding processes with larger deposition volumes, such as submerged arc welding [7–10] and tandem arc welding [11–13] with a large diameter of filler metal or multiple filler metals have been proposed. However, these processes often require high welding currents to achieve high deposition rates, which may deteriorate joint properties through grain coarsening adjacent to the fusion boundary in the heat-affected zone [14–16].

Several researchers have proposed combining hot-wire insertion with several main heat sources, such as in hot wire with laser welding [17–22] and hot wire with ultra-high-speed gas tungsten arc welding [23], which offer promising deposition volumes of hot-wire insertion. Although the deposition volume can be increased, the groove (edge) preparation and a more precious joint configuration are required. The combination of GMAW and

hot-wire feeding has since been proposed and used to increase productivity and process tolerances [24,25]. In a recent study, the full penetration of a butt-joint single-V groove in a 36 mm thick steel plate was achieved with only four weld passes [26]. Moreover, the study revealed the precedence of molten metal under the limitation of the total deposition volume, which depended on the bead width (gap size) of the butt-joint single-V groove weld. Another study suggested that increasing the welding speed not only reduced heat input but also increased the controllability of the arc at a high current and affected the weld bead shape [27]. Notably, hot-wire GMAW has promising controllability of the molten pool formation with less required heat input. The authors thus propose an optimized hot-wire GMAW for creating a single-pass weld on thick steel plates of square butt joints without edge preparation.

The present study investigates the limitations of conventional GMAW and optimizes the welding conditions of hot-wire GMAW to achieve single-pass welding on a square butt joint of 15 mm thick steel plates. To achieve this goal, the effect of the hot-wire fraction on the quality of the welded joint is investigated. The welding quality is monitored using a high-speed camera, and the weld bead geometry on an etched cross section is measured in detail. Furthermore, the power consumption and arc time are calculated and compared with those of conventional GMAW to demonstrate the energy savings and increased productivity associated with hot-wire GMAW.

2. Materials and Methods

2.1. Materials

A square butt joint of JIS-G3101-SS400 with as-cut surfaces having a length of 350 mm, width of 80 mm, and thickness of 15 mm was assembled with a 9 mm thick backing plate for the experiment as shown in Figure 1. Two root gaps, 5 and 10 mm in width, were used. The filler metal used for GMAW was a JIS-Z3312-YGW11 (G49A0UC11) solid wire with a diameter of 1.4 mm, whereas the same filler wire but with a different diameter of 1.2 mm was used for the hot wire. The chemical compositions of the materials used in the experiment are given in Table 1.

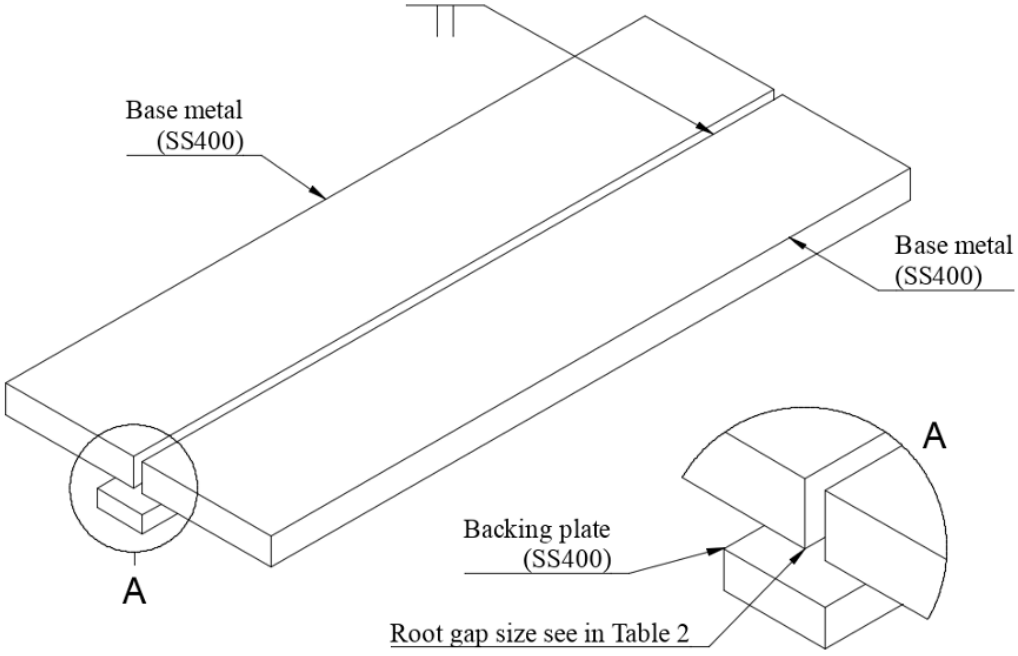


Figure 1. Joint configurations. (Root gap size see in Table 2).

Table 1. Chemical compositions of G3101-SS400 and Z3312-YGW11 (wt%).

Element	C	Si	Mn	P	S	Ti + Zr	Fe
Base metal	0.26	0.40	-	0.04	0.05	-	Bal.
Filler metal	0.08	0.51	1.10	0.01	0.01	0.05	Bal.

Table 2. Conditions of solo GMAW.

Parameters	Initial Condition	Larger Gap Condition	Faster Speed Condition
Gap size, mm	5	10	5
Travel speed, cm/min (mm/s)	30 (5)		60 (10)
Welding current, A	300–500		
Arc voltage, V	38		
Gas flow rate, L/min	25		
Contact tip to work distance, mm	30		

2.2. Experimental Setup

Figure 2a is a schematic of the experimental setup of the solo GMAW process. Industrial-grade CO_2 was used as the shielding gas. The GMAW torch was placed perpendicular to the welding direction and backing plate. Figure 2b shows the combination of the GMAW and hot wire with a 10 mm delay of the hot-wire feeding position in the welding direction. The distance from the contact tip to the workpiece and the distance of the power supply were maintained at 30 and 100 mm, respectively. The hot-wire feeding angle was fixed at 70 degrees relative to the backing plate.

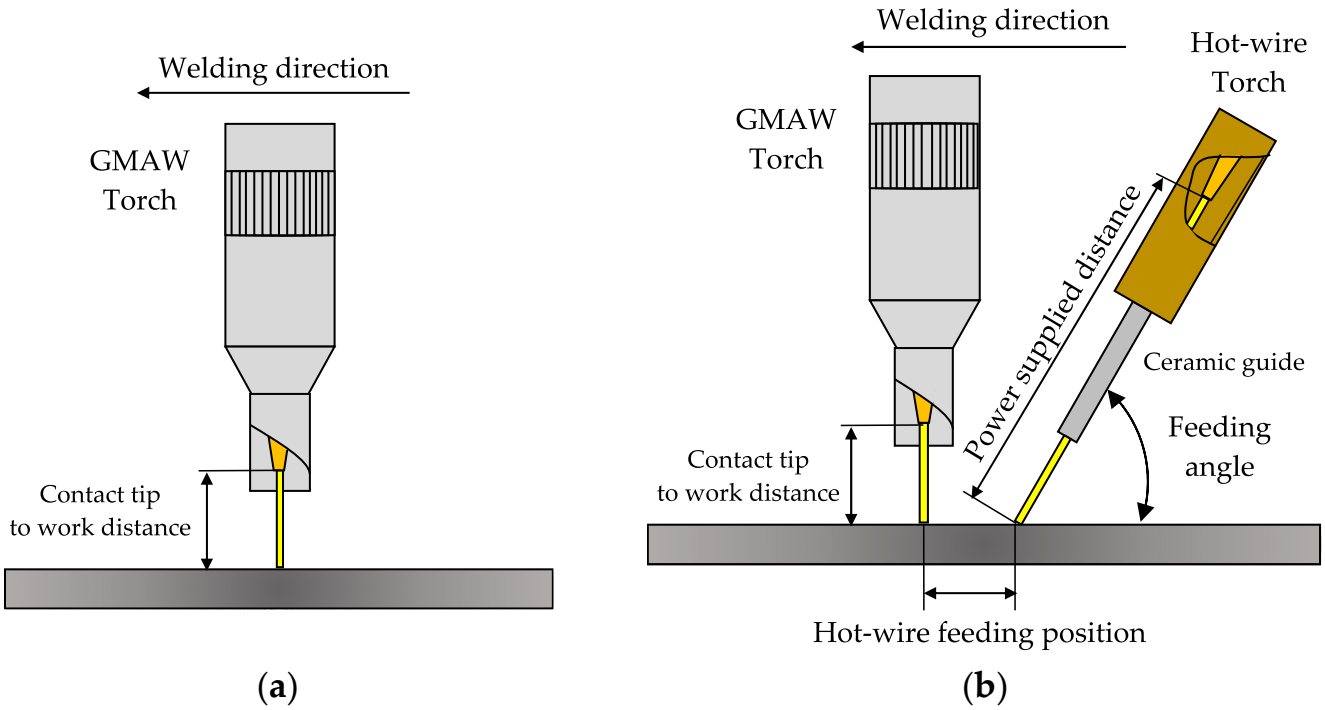


Figure 2. Welding experimental setups: (**a**) schematic of solo GMAW and (**b**) schematic of hot-wire GMAW.

Initially, GMAW was performed without hot-wire insertion to determine process capabilities and limitations. Table 2 gives the welding conditions for the solo GMAW experiment. To investigate the effect of the welding current on the weld bead profile and

arc position on the square butt joint, the welding current was increased from 300 to 500 A in intervals of 50 A while other parameters, such as an arc voltage of 38 V and travel speed of 30 cm/min, were held constant under the initial condition with the 5 mm gap. The wire feeding speed (WFS) was measured and the deposition rate of the GMAW was calculated at the different applied welding currents. Subsequently, additional experiments for a larger gap of 10 mm and a constant travel speed of 30 cm/min (5 mm/s) (larger gap condition) and a faster welding speed of 60 cm/min (10 mm/s), and a constant gap size of 5 mm (faster speed condition) were conducted to determine the limitations of the GMAW process.

The arc phenomenon and molten pool formation were observed using a high-speed camera. A band-pass filter with a transmission wavelength of 810 ± 10 nm was attached to an optical lens. A shutter speed of 1/1000 s and a frame rate of 500 fps was adopted. The resulting welds were cross-sectionally cut, polished, and etched with 3% nitric acid. Subsequently, the weld geometry was observed. Figure 3 shows measured parameters of the weld geometry, such as the fusion area (A_f), depth of penetration (D_p), maximum width (W_{max}), and height (H_{wmax}), on the obtained welded cross section.

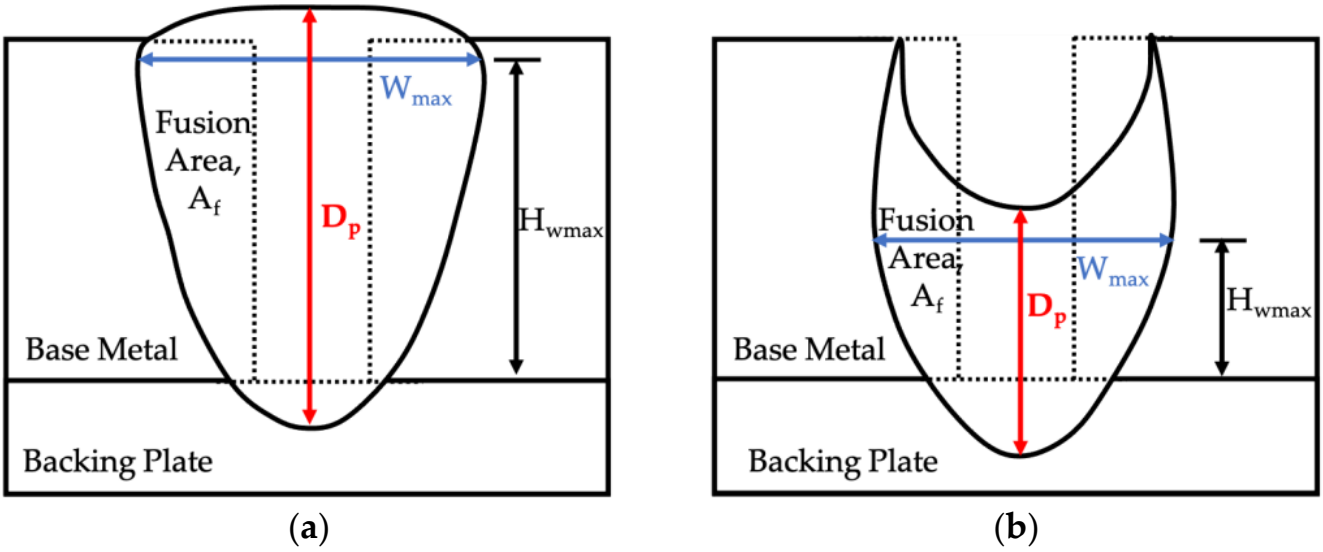


Figure 3. Measured parameters on the obtained welded cross section: (**a**) weld geometry parameters for the underfill condition and (**b**) weld geometry parameters for the full-penetration condition.

2.3. Calculation of the Optimal Hot-Wire Current

The hot wire must be smoothly and continuously fed into the molten pool to obtain an exact deposition volume. Several studies have provided simple calculations with which to derive an optimal hot-wire current that relates to the hot-wire feeding speed [23,26,28]. The power supply distance of 100 mm was divided into segments of 0.1 mm (L). The temperature increment on a segment (ΔT) in degrees Celsius is given by

$$\Delta T = Q/C(T) \times m(T) \times L \times \pi r^2 \quad (1)$$

where C(T) is the temperature-dependent specific heat in J/kg·°C, m(T) is the temperature-dependent density in kg/m^3, and r is the radius of the hot wire filler metal in mm.

Q is the net heat increase is the difference between the generated heat by the Joule heating into the segment (Q_{in}) in J and the heat loss from the segment (Q_{out}) in J, which is given by

$$Q = Q_{in} - Q_{out} \quad (2)$$

where

$$Q_{in} = R(T) \times I^2 \times t \quad (3)$$

where R(T) is the temperature-dependent resistance of the filler metal in Ω, I is the hot-wire current in A, and t is the heating time through the segment in s.

The temperature-dependent resistance R(T) of the segment is expressed as

$$R(T) = (R_C + \rho(T)) \times L/\pi r^2 \quad (4)$$

where ρ(T) is the temperature-dependent specific electrical resistivity in Ω·m, and R_c is the contact resistance in Ω.

The heating time through a segment is

$$t = D \times 60 \times L/v_{HW} \quad (5)$$

where D is the duty cycle of the wire heating (normally set at 50%), and V_{HW} is the hot wire feeding speed in mm/s.

The heat loss (Q_{out}) in J is expressed as

$$Q_{out} = h \times \pi r^2 \times \Delta T \quad (6)$$

where h is the comprehensive heat loss coefficient in W/m^2 K

The temperature increment on a segment (ΔT) is the difference between the temperature of filler metal (T_W) and ambient temperature (T_A) in °C given as

$$\Delta T = T_W - T_A \quad (7)$$

Substituting Equations (2)–(7) into Equation (1), a simple equation is derived to calculate the temperature increment on the hot-wire segment:

$$(T_W - T_A) = \frac{I^2}{v_{HW}} \times \frac{60 \times L \times D \times (R_c + \rho(T))}{\pi^2 \times r^2 \times C(T) \times m(T)} - \frac{h \times (T_W - T_A)}{C(T) \times m(T) \times L} \quad (8)$$

Equation (8) is used to obtain the optimal hot-wire current (I) when the wire temperature at the tip equals the melting temperature.

2.4. Definition of the Hot-Wire Fraction

The hot-wire insertion volume is used as an independent deposition metric and increased to increase the total deposition volume. The hot-wire fraction representing this effect is expressed as

$$\%HW = \frac{V_{HW}}{(V_{HW} + V_{GMAW})} \times 100, \quad (9)$$

where %HW is the hot-wire fraction in percent, V_{HW} is the deposition rate of hot-wire mm^3/s, and V_{GMAW} is the deposition rate of GMAW in mm^3/s. V_{GMAW} is the wire feeding speed of GMAW in mm/s, which is given by

$$V_{HW} = \pi \times 1.2^2 \times v_{HW} \quad (10)$$

$$V_{GMAW} = \pi \times 1.4^2 \times v_{GMAW} \quad (11)$$

Substituting Equations (10) and (11) into Equation (9) to calculate the percentage of hot-wire fraction of the total deposition rate.

2.5. Calculation of the Power Consumption

A data acquisition system operating at 5000 Hz was used to record the welding current in A, arc voltage in V, hot-wire current in A, and hot-wire voltage in V. The total power consumption (P_{total}) is

$$P_{total} = (P_{GMAW} + P_{HW}) \times t_{arc} \quad (12)$$

where

$$P_{GMAW} = \frac{(I_{GMAW1} \times V_{GMAW1}) + (I_{GMAW2} \times V_{GMAW2}) + \ldots + (I_{GMAWn} \times V_{GMAWn})}{5000}, \quad (13)$$

$$P_{HW} = \frac{\left(\sqrt{I_{HW1}^2} \times \sqrt{V_{HW1}^2}\right) + \left(\sqrt{I_{HW2}^2} \times \sqrt{V_{HW2}^2}\right) + \ldots + \left(\sqrt{I_{HWn}^2} \times \sqrt{V_{HWn}^2}\right)}{5000}. \quad (14)$$

Here, P_{GMAW} is the power used in GMAW in kJ, PHW is the power used in hot wire insertion (kJ), I_{GMAW} is the welding current (A), V_{GMAW} is the arc voltage (volt), I_{HW} is the hot-wire current (A), and V_{HW} is the hot-wire voltage (volt), and t_{arc} is arc time in s.

3. Capability of GMAW

3.1. Relationship between the Welding Current and WFS

Figure 4 presents the relationship between the welding current and measured WFS in solo GMAW. It is seen that despite fluctuations in the welding current, the constant-voltage GMAW welding power source maintains a nearly constant arc length, resulting in a proportional relationship between the welding current and WFS [29]. This result reveals the necessity of increasing the welding current to obtain a larger deposition volume, leading to more heat input to the joint and ultimately grain coarsening adjacent to the fusion line and worse joint properties. This highlights the limitation of conventional GMAW in achieving desired deposit volumes and emphasizes the importance of independent supplemental deposition techniques that do not rely on the welding current.

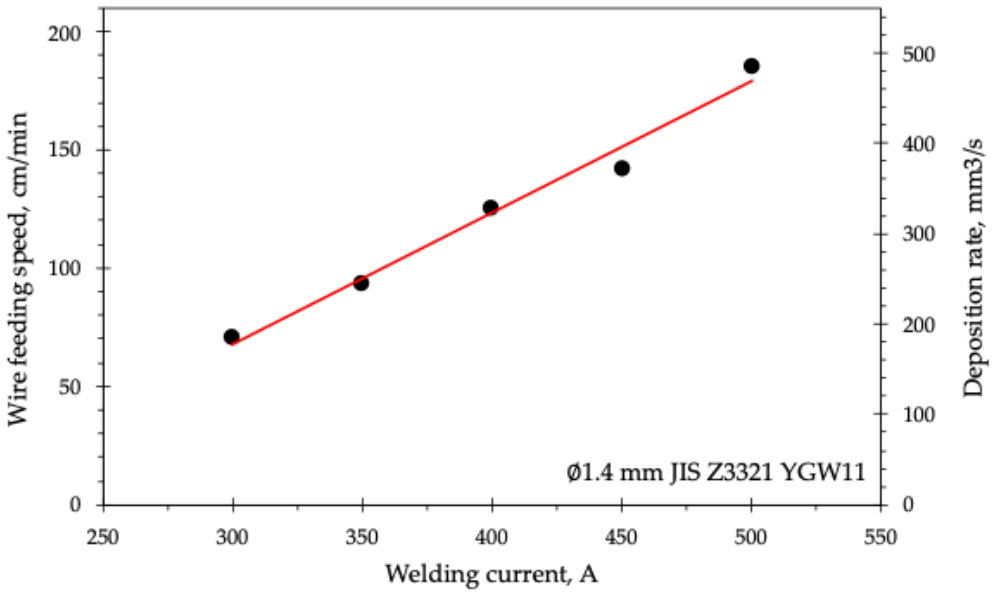


Figure 4. Relationship between the welding current, wire feeding speed, and deposition rate.

3.2. Arc Phenomenon, Bead Appearance, and Weld Geometry

The study examined the effect of varying the welding current from 300 to 500 A under three different sets of conditions, as previously given in Table 2. Figure 5a presents the

captured high-speed images, weld bead appearances, and cross sections when conventional GMAW was applied to the 5 mm gap of the square butt joint with a welding speed of 30 cm/min (i.e., the initial set of conditions). The captured high-speed images show different arc positions relating to the height of the molten pool. As the welding current was increased, the arc moved upward in the depth direction, resulting in a shorter stick-out distance of the filler metal. A sound weld bead shape could not be achieved under the initial conditions. A welding current lower than 400 A resulted in an insufficient depth of penetration with incomplete fusion; i.e., underfilling of the weld bead with a cone-shaped fusion area. However, increasing the welding current helped to overcome incomplete fusion, changing the shape of the fusion area from a cone to a rectangle. Similar behavior was also observed by Nakamura et al. [30].

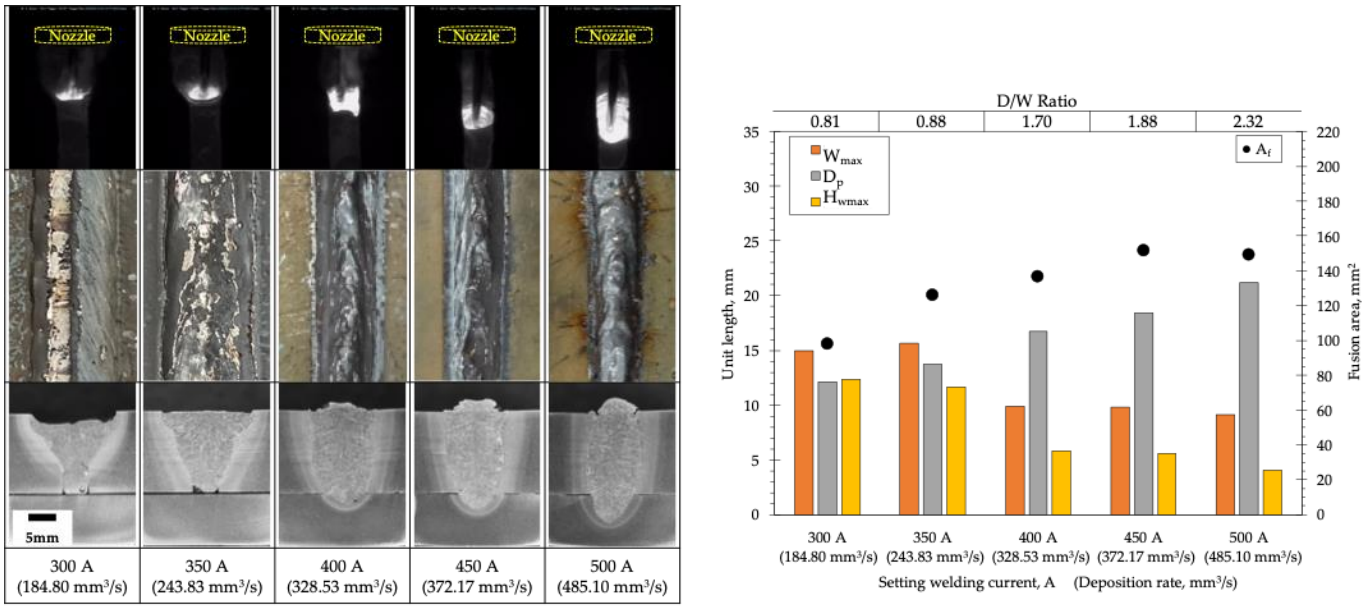


Figure 5. Effect of the welding current in solo GMAW for a 5 mm gap and a welding speed of 30 cm/min: (**a**) arc behavior, weld bead appearance, and cross-sectional analysis and (**b**) weld profile measurement.

Figure 5b illustrates that increasing the welding current not only provided a larger deposition volume but also affected the weld bead geometry. Increasing the welding current resulted in a narrower maximum weld width (W_{max}) and larger depth of penetration (D_p). The height of the maximum weld width position (H_{wmax}) represents the arc position in this experiment, and Figure 5b shows that the arc was positioned deeper in the thickness direction as the welding current increased. The depth-to-width (D/W) ratio has been used to explain the change in the shape of a weld profile and its sensitivity to hot cracking [31]. A welding current between 400 to 500 A provided similar fusion area sizes (A_f) but with a large difference in the D/W ratio. In general, a high D/W ratio in solo GMAW led to solidification cracking and a non-smooth bead appearance as shown in Figure 5a.

In the following welding experiments, similar deposition rates were achieved for the same welding speed of 0.3 m/min, but with the root gap increasing from 5 to 10 mm. Figure 6a presents the images captured during welding, the appearances of weld beads, and the cross sections obtained for comparable deposition rates. The larger root gap allowed the generation of a bigger molten pool at the root, even when applying the lowest welding current (300 A) in this experiment. Despite only increasing the gap, a deposition volume sufficient for single-pass welding could not be achieved, although the precedence of molten metal was suppressed. Figure 6b shows that H_{wmax} decreased as the welding current increased, and the arc was positioned deeply in the thickness direction, leading to a high

D/W ratio. However, the yellow bar indicates only a positive value, which means that the arc was in the region of the backing plate. When the welding current exceeded 450 A, the obtained D_p exceeded the thickness of the base metal. These results suggest that if the arc can be shifted to the upper side of the joint, unnecessary penetration can be reduced, and a single-pass welded joint can be obtained.

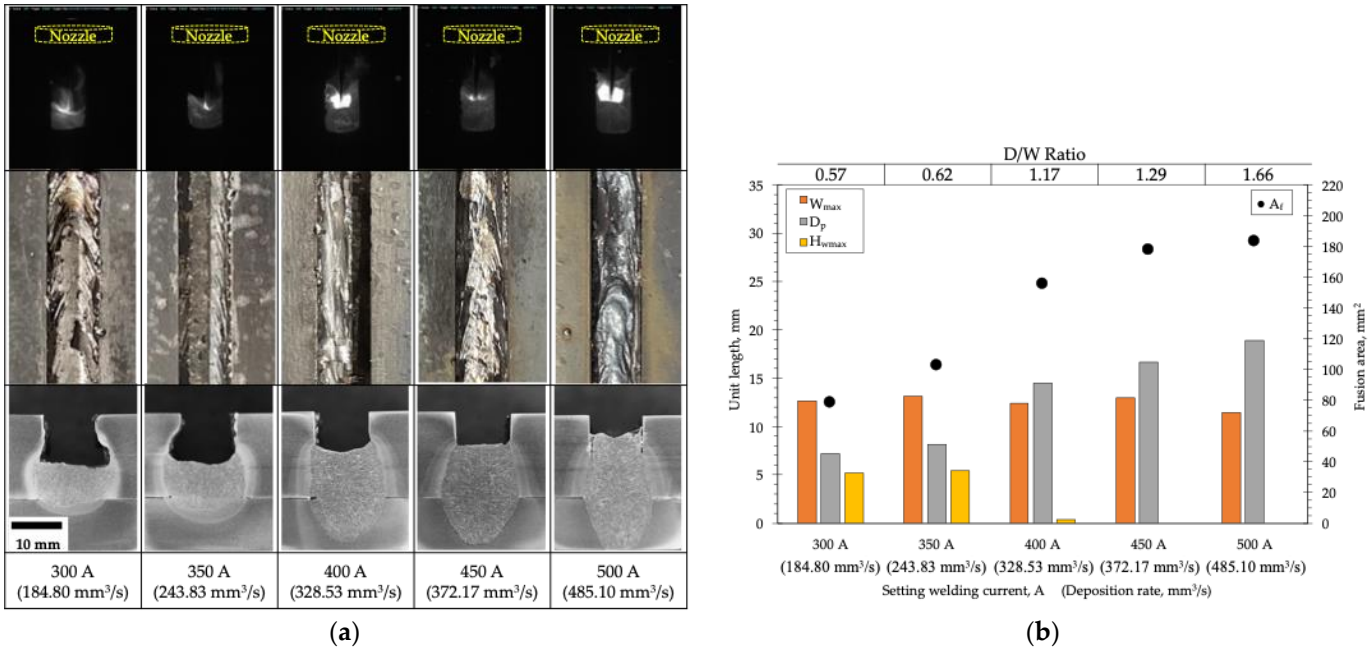


Figure 6. Effects of the welding current for a 10 mm gap and a travel speed of 30 cm/min: (**a**) arc behavior, weld bead appearance, and cross-sectional analysis and (**b**) weld profile measurement.

Another experiment was conducted where a similar deposition rate was used for the 5 mm root gap but the welding speed was increased from 30 to 60 cm/min. Figure 7a presents the captured images, weld bead appearances, and macro-etched cross sections. When using a welding current of 300 A, the molten pool was generated at the upper side of the gap, leading to incomplete fusion on the bottom side. Thus, the D/W ratio and D_p could not be determined under the conditions. The welding speed is the most dominant factor of heat input [14,27]. The halving of the heat input due to the doubling of the welding speed resulted in a smaller molten pool as seen in the captured images. In this experiment, all welding currents provided an underfill weld bead (insufficient deposition volume) and poor weld geometry (high D/W ratio), which resulted in solidification cracking at the center of the weld metal perpendicular to the direction of solidification. Figure 7b shows a similar trend for H_{wmax}, which decreased with increasing welding current compared with both prior experiments. A similar behavior was observed for W_{max}, which decreased with increasing welding current.

In summary, the three experiments revealed the limitation of conventional GMAW, namely that the deposition rate is restricted by the welding current. This series of experiments showed that single-pass welding on a square butt joint of 15 mm thick steel plates could not be achieved through solo conventional GMAW. To overcome this drawback, an independent additional volume from the hot wire was used in further investigation.

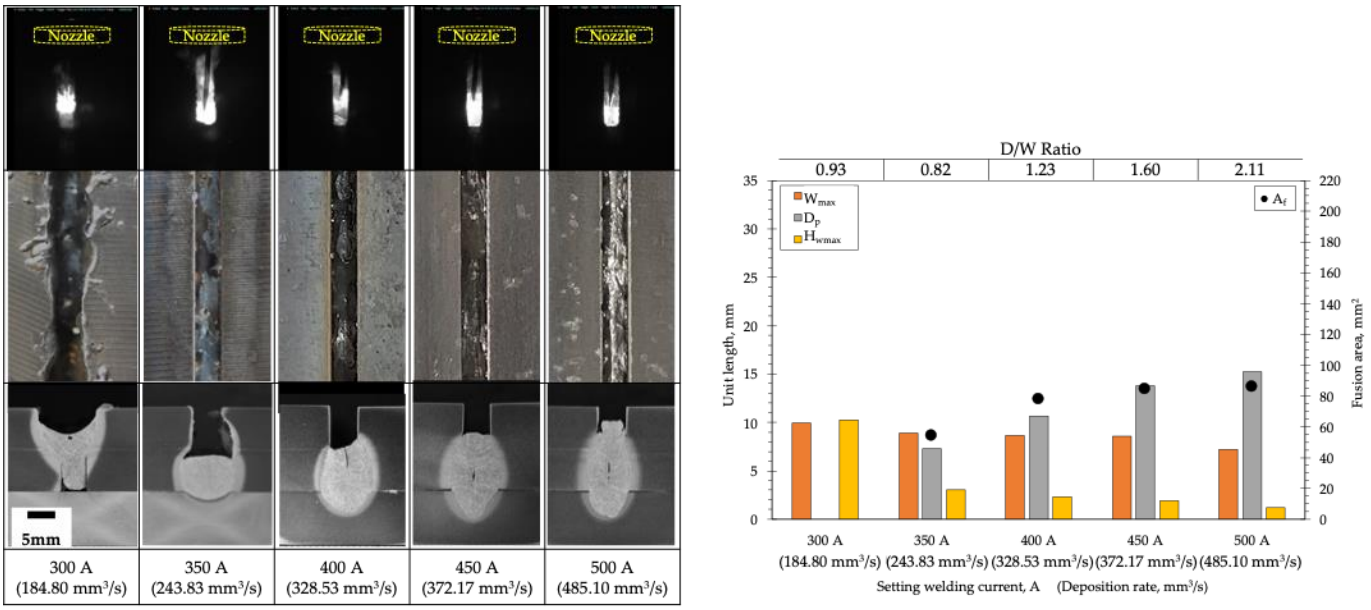


Figure 7. Effects of the welding current for a 5 mm gap and a travel speed of 60 cm/min: (**a**) arc behavior, weld bead appearance, and cross-sectional analysis and (**b**) weld profile measurement.

4. Capability of the Hot-Wire GMAW Process

4.1. Relationship between the Hot-Wire Current and Hot-Wire Feeding Speed

To ensure continuous hot-wire feeding, the appropriate hot-wire current was determined according to the wire feeding speed. Figure 8 depicts the behaviors observed for a 1.2 mm diameter hot wire fed at 10 m/min. The measured optimal hot-wire current indicated by red circles provided an appropriate feed. An insufficient hot-wire current, as indicated by the red square, can result in the formation of unmelted filler metal in a molten pool, which can push the molten metal forward. Meanwhile, an excessive hot-wire current, as shown by the red cross, can lead to the interruption and meltdown of wire feeding and thus negatively affect the deposition rate and weld quality. The correlation between the optimal hot-wire current and hot-wire feeding speed was established and used in the subsequent experiment. This correlation is essential for achieving a stable wire feed and maintaining the desired weld quality in single-pass welding.

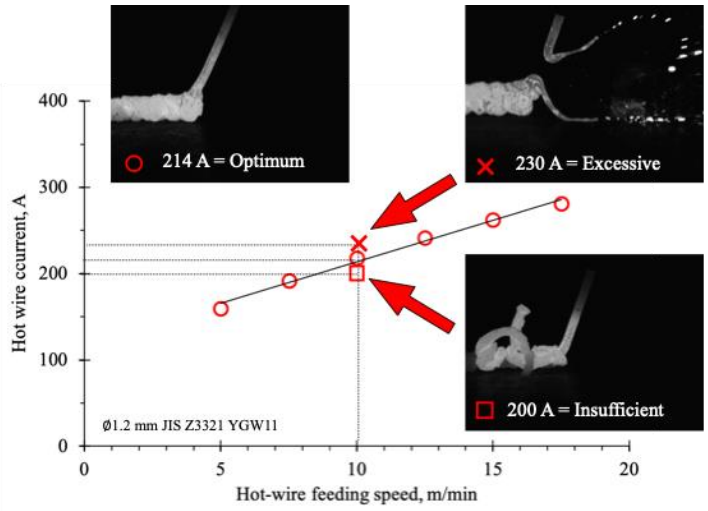


Figure 8. Correlation between the optimal hot-wire current and hot-wire feeding speed.

4.2. Effect of the Hot-Wire Fraction on Weld Formation and Obtained Weld Geometry

Hot-wire insertion can be controlled independently from the welding current as an independent fraction volume, greatly affecting the total deposition volume. The hot-wire fraction was increased to achieve sufficient deposition rates for the larger gap and faster welding speed conditions. For conventional GMAW in the prior session, a welding current of 500 A resulted in an excessive deposition volume and an overly strong and unstable arc, whereas a welding current below 400 A did not provide a sufficient deposition volume even with hot-wire insertion. Therefore, a constant welding current of 450 A was chosen to optimize the single-pass welding conditions. The hot-wire fraction was varied to analyze the weld pool formation and the obtained weld geometry. Increasing the fraction in the total deposition volume enabled single-pass welding under the specified conditions.

Figure 9a shows the images captured during welding and cross sections for a 10 mm gap and a welding speed of 30 cm/min. The increase in the hot-wire fraction lifted upward the central position of the weld bead toward the plate surface, resulting in the generation of the molten pool on the upper side of the groove. Although the total deposition volume increased with the hot-wire fraction, the arc force was sufficient to maintain the molten pool shape and penetration in the bottom region. Figure 9b presents the parameters of the measured geometry of the weld bead. W_{max} and D_p remained approximately constant whereas H_{wmax}, representing the arc position, increased with the deposition rate. The D/W ratios emphasized the similarity of the weld geometry. The hot-wire fraction can thus be used to adjust the position of the weld bead and reduce unnecessary penetration. Sound joint conditions were achieved at a hot-wire fraction of 43.18%.

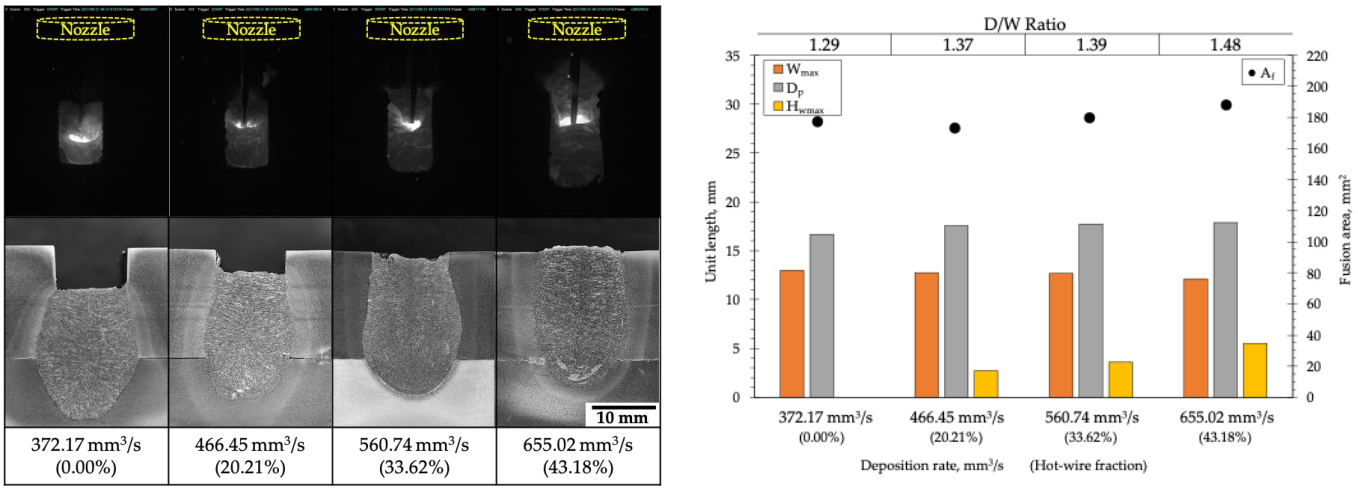


Figure 9. Effects of the hot-wire fraction for a 10 mm gap and travel speed of 30 cm/min: (**a**) arc behavior and cross-sectional analysis and (**b**) weld profile measurements.

A similar experiment was conducted for a 5 mm gap and a travel speed of 60 cm/min. Figure 10a shows that the position of the arc changed as the hot-wire fraction increased. For a constant GMAW fraction, the arc shifted toward the top surface with an increase in the hot-wire fraction up to 43.18%. This is strong evidence that the hot-wire fraction can be used to control the arc position and enlarge the process tolerance. Thus, single-pass welding of a 15 mm square butt joint could be achieved even at a travel speed of 60 cm/min. Figure 10b illustrates a trend in the weld geometry similar to that in the prior experiment, with an obvious increase in H_{wmax} with the deposition rate. Notably, solidification cracking that first occurred when conventional GMAW was applied shifted position as the hot-wire fraction increased. In addition, the crack disappeared at a hot-wire fraction of 43.18%, and the conditions provided a sound joint without defects.

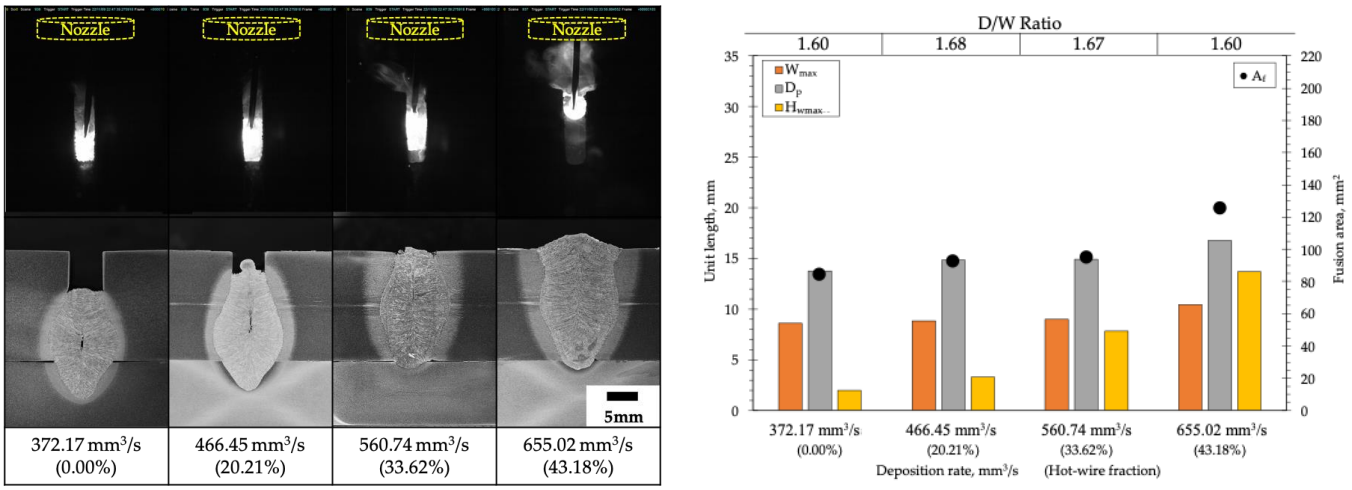


Figure 10. Effects of the hot-wire fraction for a 5 mm gap and travel speed of 60 cm/min: (**a**) arc behavior and cross-sectional analysis and (**b**) weld profile measurements.

5. Production Efficiency and Power Consumption

5.1. Production Efficiency

Figure 11 presents a reduction in the arc time when using hot-wire insertion compared with using conventional GMAW. The adoption of the proposed process resulted in an 83.3% reduction in the arc time at the same travel speed. At a travel speed of 60 cm/min, single-pass welding had a remarkable 91.67% reduction in arc time. These reductions in arc time, represented by gray bars in the figure, can be considered a measure of production efficiency. The use of hot-wire insertion led to a notable increase in production efficiency. By reducing the required number of weld passes from six to one, production efficiency increased by a factor of approximately 5 at the same travel speed of 30 cm/min. Under optimized conditions of a 5 mm gap and a travel speed of 60 cm/min, the production efficiency of the proposed method was approximately 11 times that of the conventional GMAW. In addition, the proposed welding process is suitable for a square groove without any preparation and with a large gap variation.

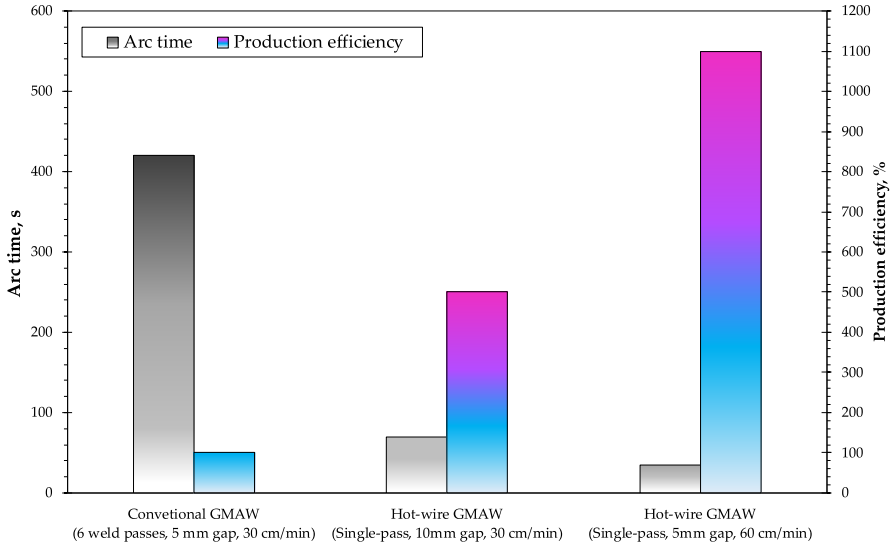


Figure 11. Comparison of the arc time and power consumption between conventional GMAW and the proposed hot-wire GMAW.

5.2. Power Consumption

Figure 12 presents the relationship between the deposition rate and power consumption for various welding processes. Conventional GMAW has limited process tolerance, with the deposition volume depending on the applied welding current and filler metal diameter [24,26]. Proposed high-current CO_2 arc welding has a high deposition rate but requires power consumption similar to that required by submerged arc welding (SAW) [3]. Increasing the diameter of the filler metal improves the deposition rate of SAW [10] but inevitably results in high power consumption. However, the adoption of hot-wire insertion led to a reduction in power consumption of 62% compared with SAW for a similar deposition volume. The proposed method is thus a sustainable-development way of achieving high deposition volume while minimizing power consumption. The optimized hot-wire current and fraction enable stable hot-wire feeding for the arc and maximize the deposition rate, making the proposed method promising for welding applications that require high productivity and energy efficiency.

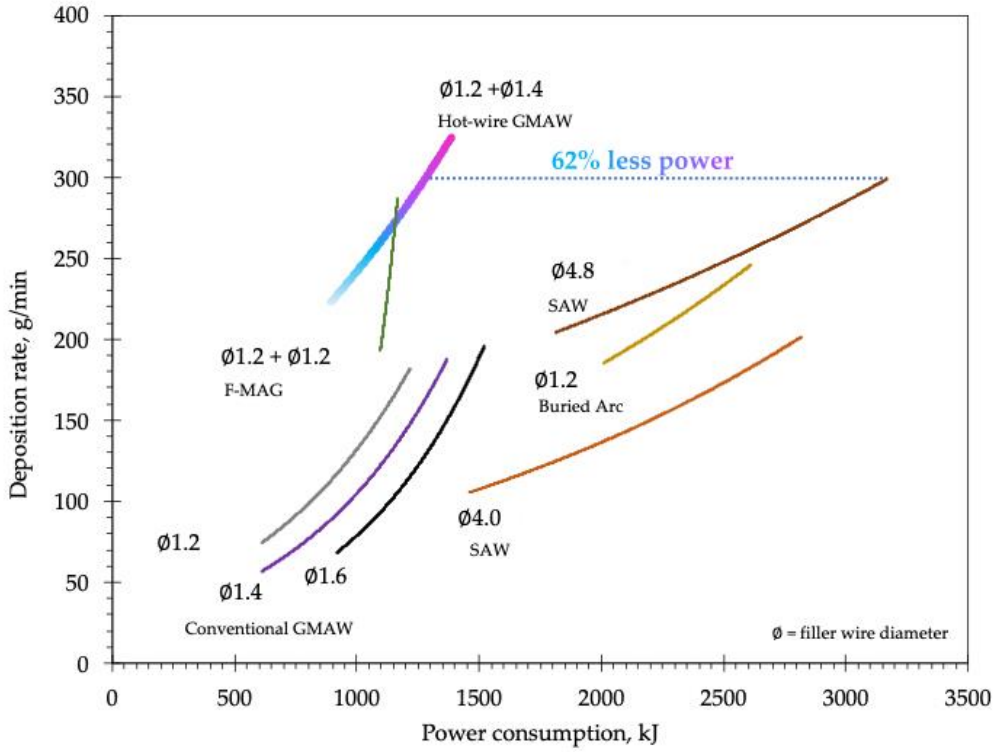


Figure 12. Relationship between the deposition rate and power consumption in various welding processes [3,4,10,24,26].

6. Conclusions

This study investigated the limitation of conventional GMAW and the use of the hot-wire fraction as a parameter for controlling the desired position of the weld metal. The results of the study show that the new approach forms a promising sound joint when optimized conditions are applied. The main results and conclusions of the study are as follows.

1. The limited process tolerance of GMAW in achieving single-pass welding was shown. Obtaining a greater deposition volume inevitably requires high heat input to the joint.
2. As the hot-wire fraction increases, the molten pool tends to form on the upper side of the joint. Unnecessary penetration is reduced, and a desired arc position is obtained, particularly for large gaps and high travel speeds.
3. The simple joint configuration can be used to achieve single-pass welding using the proposed process.

4. The independent deposition volume due to hot-wire insertion increases the total deposition volume without requiring more welding current. Single-pass welding at a welding speed of 60 cm/min resulted in an 81.25% decrease in power consumption.
5. The productivity increases with decreasing arc time. The proposed approach requires 91.67% less arc time compared with conventional GMAW.
6. The use of the hot wire reduces the occurrence of solidification cracks in the welded joint.

However, further research is needed to optimize the hot-wire fraction and other process parameters and thus achieve the best possible welding results for specific applications.

Author Contributions: Conceptualization, N.S. and M.Y.; methodology, N.S.; software, N.S.; validation, N.S. and M.Y.; investigation, N.S.; resources, M.Y.; data curation, N.S.; writing—original draft preparation, N.S.; writing—review and editing, N.S. and M.Y.; visualization, N.S.; supervision, M.Y.; project administration, M.Y.; funding acquisition, M.Y. All authors have read and agreed to the published version of the manuscript.

Funding: This work was supported by JSPS KAKENHI Grant Number 21H01548.

Data Availability Statement: Not applicable.

Acknowledgments: We express our sincere gratitude to Kanon Nakamura for their invaluable contributions and support throughout this project.

Conflicts of Interest: The authors declare no conflict of interest.

References

1. Masmoudi, F.; Bouaziz, Z.; Hachicha, W. Computer-aided cost estimation of weld operations. *Int. J. Adv. Manuf. Technol.* **2007**, *33*, 298–307. [CrossRef]
2. Chayoukhi, S.; Bouaziz, Z.; Zghal, A. Cost estimation of joints preparation for GMAW welding process using feature model. *J. Mater. Process. Technol.* **2008**, *199*, 402–411. [CrossRef]
3. Tsuyama, T.; Yuda, M.; Nakai, K. Effects of hot wire on mechanical properties of weld metal using gas-shield arc welding with CO_2 gas. *Weld World* **2014**, *58*, 77–83. [CrossRef]
4. Baba, H.; Era, T.; Ueyama, T.; Tanaka, M. Single pass full penetration joining for heavy plate steel using high current GMA process. *Weld World* **2017**, *61*, 963–969. [CrossRef]
5. Baba, H.; Kadota, K.; Era, T.; Ueyama, T.; Maeshima, M.; Kadoi, K.; Inoue, H.; Tanaka, M. Single-pass full-penetration welding for thick stainless steel using high-current GMAW. *Q. J. Jpn. Weld. Soc.* **2021**, *39*, 39–50. [CrossRef]
6. Wu, C.S.; Hu, Z.H.; Zhong, L.M. Prevention of humping bead associated with high welding speed by double-electrode gas metal arc welding. *Int. J. Adv. Manuf. Technol.* **2012**, *63*, 573–581. [CrossRef]
7. Gunaraj, V.; Murugan, N. Application of response surface methodology for predicting weld bead quality in submerged arc welding of pipes. *J. Mater. Process. Technol.* **1991**, *88*, 266–275. [CrossRef]
8. Murugan, N.; Gunraj, V. Prediction and control of weld bead geometry and shape relationships in submerged arc welding of pipes. *J. Mater. Process. Technol.* **2005**, *168*, 478–487. [CrossRef]
9. Wu, Y.; Yuan, X.; Kaldre, I.; Zhong, M.; Wang, Z.; Wang, C. TiO_2-assisted microstructural variations in the weld metal of EH36 shipbuilding steel subject to high heat input submerged arc welding. *Metall. Mater. Trans. B* **2023**, *54*, 50–55. [CrossRef]
10. Tsuyama, T.; Nakai, K.; Tsuji, T. Development of submerged arc welding method using hot wire. *Weld World.* **2014**, *58*, 713–718. [CrossRef]
11. Ueyama, T.; Ohnawa, T.; Tanaka, M.; Nakata, K. Effects of torch configuration and welding current on weld bead formation in high speed tandem pulsed gas metal arc welding of steel sheets. *Sci. Technol. Weld. Join.* **2005**, *10*, 750–759. [CrossRef]
12. Ueyama, T.; Ohnawa, T.; Tanaka, M.; Nakata, K. Occurrence of arc interaction in tandem pulsed gas metal arc welding. *Sci. Technol. Weld. Join.* **2007**, *12*, 523–529. [CrossRef]
13. Liu, G.; Han, S.; Tang, X.; Cui, H. Effects of torch configuration on arc interaction behaviors and weld defect formation mechanism in tandem pulsed GMAW. *J. Manuf. Process.* **2021**, *62*, 729–742. [CrossRef]
14. Kou, S. Work-Hardened Materials. In *Welding Metallurgy*, 2nd ed.; John Wiley & Sons, Inc.: Hoboken, NJ, USA, 2003; pp. 343–351.
15. Li, B.; Liu, Q.; Jia, S.; Ren, Y.; Yang, P. Effect of V content and heat input on HAZ softening of deep-sea pipeline steel. *Materials* **2022**, *15*, 794. [CrossRef]
16. Sun, L.; Li, H.; Zhu, L.; Liu, Y.; Hwang, J. Research on the evolution mechanism of pinned particles in welding HAZ of Mg treated shipbuilding steel. *Mater. Des.* **2020**, *192*, 108670. [CrossRef]
17. Li, R.; Wang, T.; Wang, C.; Yan, F.; Shao, X.; Hu, X.; Li, J. A study of narrow gap laser welding for thick plates using the multi-layer and multi-pass method. *Opt. Laser Technol.* **2014**, *64*, 172–183. [CrossRef]
18. Acherjee, B. Hybrid laser arc welding. *Opt. Laser Technol.* **2018**, *99*, 67–71. [CrossRef]

19. Hammad, A.; Churiaque, C.; Sánchez-Amaya, J.M.; Abdel-Nasser, Y. Experimental and numerical investigation of hybrid laser arc welding process and the influence of welding sequence on the manufacture of stiffened flat panels. *J. Manuf. Process.* **2021**, *61*, 527–538. [CrossRef]
20. Wei, H.; Zhang, Y.; Tan, L.; Zhong, Z. Energy efficiency evaluation of hot-wire laser welding based on process characteristic and power consumption. *J. Clean. Prod.* **2015**, *87*, 255–262. [CrossRef]
21. Phaoniam, R.; Shinozaki, K.; Yamamoto, M.; Kadoi, K.; Tsuchiya, S.; Nishijima, A. Development of a highly efficient hot-wire laser hybrid process for narrow-gap welding-welding phenomena and their adequate conditions. *Weld World* **2013**, *57*, 607–613. [CrossRef]
22. Kisielewicz, A.; Thalavai Pandian, K.; Sthen, D.; Hagqvist, P.; Valiente Bermejo, M.A.; Sikström, F.; Ancona, A. Hot-wire laser-directed energy deposition: Process characteristics and benefits of resistive pre-heating of the feedstock wire. *Metals* **2021**, *11*, 634. [CrossRef]
23. Shinozaki, K.; Yamamoto, M.; Mitsuhata, K.; Nakashima, T.; Kanazawa, T.; Arashin, H. Bead formation and wire temperature distribution during ULTRA-HIGH-SPEED GTA WELDING using pulse-heated hot-wire. *Weld World* **2012**, *55*, 12–18. [CrossRef]
24. Wonthaisong, S.; Shinohara, S.; Shinozaki, K.; Phaoniam, R.; Yamamoto, M. High-efficiency and low-heat-input CO_2 arc welding technology for butt joint of thick steel plate using hot wire. *Q. J. Jpn. Weld. Soc.* **2020**, *38*, 164–170. [CrossRef]
25. Spaniol, E.; Trautmann, M.; Ungethüm, T.; Hertel, M.; Füssel, U.; Henckell, P.; Bergmann, J.P. Development of a highly productive GMAW hot wire process using a two-dimensional arc deflection. *Weld World* **2020**, *64*, 873–883. [CrossRef]
26. Suwannatee, N.; Wonthaisong, S.; Yamamoto, M.; Shinohara, S.; Phaoniam, R. Optimization of welding conditions for hot-wire GMAW with CO_2 shielding on heavy-thick butt joint. *Weld World* **2022**, *66*, 833–844. [CrossRef]
27. Marumoto, K.; Tamata, H.; Fujinaga, A.; Takahashi, T.; Yamamoto, H.; Choi, J.; Yamamoto, M. Bead shape control in high-speed fillet welding using hot-wire GMA laser hybrid welding technology. *Weld World* **2023**, *67*, 1259–1266. [CrossRef]
28. Zhu, S.; Nakahara, Y.; Yamamoto, M.; Shinozaki, K.; Aono, H.; Ejima, R. Additive manufacturing phenomena of various wires using a hot-wire and diode laser. *Weld World* **2022**, *66*, 1315–1327. [CrossRef]
29. Holliday, D.B.; Dull, R.M.; Hartman, D.K.; Wright, D.A. Chapter 4—Gas Metal Arc Welding. In *Welding Handbook*, 9th ed.; O'Brien, A., Ed.; American Welding Society: Miami, FL, USA, 2004; Volume 2, pp. 148–197.
30. Nakamura, T.; Hiroaka, K. Ultranarrow GMAW process with newly developed wire melting control system. *Sci. Technol. Weld. Join.* **2001**, *6*, 355–362. [CrossRef]
31. Phaoniam, R.; Shinozaki, K.; Yamamoto, M.; Kadoi, K.; Nishijima, A.; Yamamoto, M. Solidification cracking susceptibility of modified 9Cr1Mo steel weld metal during hot-wire laser welding with a narrow gap groove. *Weld World* **2014**, *58*, 469–476. [CrossRef]

Disclaimer/Publisher's Note: The statements, opinions and data contained in all publications are solely those of the individual author(s) and contributor(s) and not of MDPI and/or the editor(s). MDPI and/or the editor(s) disclaim responsibility for any injury to people or property resulting from any ideas, methods, instructions or products referred to in the content.